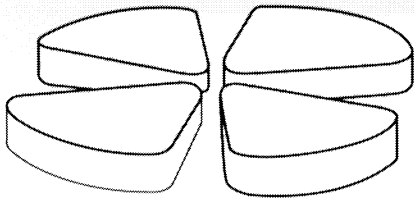


# GANIL

GRAND ACCELERATEUR NATIONAL D'IONS LOURDS - CAEN  
LABORATOIRE COMMUN IN2P3 (CNRS) - D.S.M. (CEA)



## Magnetic Moment of the Fragmentation-Aligned $^{61}\text{Fe}(9/2^+)$ Isomer.

I. Matea,<sup>1</sup> G. Georgiev,<sup>1</sup> J.M. Daugas,<sup>2</sup> M. Hass,<sup>3</sup> G. Neyens,<sup>4</sup> R. Astabatyán,<sup>5</sup> L.T. Baby,<sup>3</sup> D.L. Balabanski,<sup>6</sup>  
G. Bélier,<sup>2</sup> D. Borremans,<sup>4</sup> F. Chappert,<sup>2</sup> M. Girod,<sup>2</sup> G. Goldring,<sup>3</sup> H. Goutte,<sup>2</sup> P. Himpe,<sup>4</sup> M. Lewitowicz,<sup>1</sup>  
S. Lukyanov,<sup>5</sup> V. Méot,<sup>2</sup> F. de Oliveira Santos,<sup>1</sup> Yu.E. Penionzhkevich,<sup>5</sup> M.-G. Porquet,<sup>7</sup> O. Roig,<sup>2</sup> and M. Sawicka<sup>8</sup>

<sup>1</sup>GANIL, BP 55027, 14076 Caen Cedex 5, France

<sup>2</sup>CEA/DIF/DPTA/PN, BP 12, 91680 Bruyères le Châtel, France

<sup>3</sup>The Weizmann Institute, Rehovot, Israel

<sup>4</sup>University of Leuven, IKS, Celestijnenlaan 200 D, 3001 Leuven, Belgium

<sup>5</sup>FLNR-JINR, Dubna, Russia

<sup>6</sup>Faculty of Physics, St. Kliment Ohridski University of Sofia, 1164 Sofia, Bulgaria.

<sup>7</sup>CSNSM, Orsay, France

<sup>8</sup>IFD, Warsaw University, Hoza 69, 00681 Warsaw, Poland

(Dated: September 24, 2004)

Submitted to *Physical Review Letters*

CERN LIBRARIES, GENEVA



CM-P00055442

GANIL P 04 07

# Magnetic Moment of the Fragmentation-Aligned $^{61}\text{Fe}(9/2^+)$ Isomer.

I. Matea,<sup>1</sup> G. Georgiev,<sup>1</sup> J.M. Daugas,<sup>2</sup> M. Hass,<sup>3</sup> G. Neyens,<sup>4</sup> R. Astabatyany,<sup>5</sup> L.T. Baby,<sup>3</sup> D.L. Balabanski,<sup>6</sup> G. Bélier,<sup>2</sup> D. Borremans,<sup>4</sup> F. Chappert,<sup>2</sup> M. Girod,<sup>2</sup> G. Goldring,<sup>3</sup> H. Goutte,<sup>2</sup> P. Himpe,<sup>4</sup> M. Lewitowicz,<sup>1</sup> S. Lukyanov,<sup>5</sup> V. Méot,<sup>2</sup> F. de Oliveira Santos,<sup>1</sup> Yu.E. Penionzhkevich,<sup>5</sup> M.-G. Porquet,<sup>7</sup> O. Roig,<sup>2</sup> and M. Sawicka<sup>8</sup>

<sup>1</sup>GANIL, BP 55027, 14076 Caen Cedex 5, France

<sup>2</sup>CEA/DIF/DPTA/PN, BP 12, 91680 Bruyères le Châtel, France

<sup>3</sup>The Weizmann Institute, Rehovot, Israel

<sup>4</sup>University of Leuven, IKS, Celestijnenlaan 200 D, 3001 Leuven, Belgium

<sup>5</sup>FLNR-JINR, Dubna, Russia

<sup>6</sup>Faculty of Physics, St. Kliment Ohridski University of Sofia, 1164 Sofia, Bulgaria.

<sup>7</sup>CSNSM, Orsay, France

<sup>8</sup>IFD, Warsaw University, Hoża 69, 00681 Warsaw, Poland

(Dated: September 24, 2004)

We report on the g factor measurement of the isomer in  $^{61}\text{Fe}$  ( $E^* = 861 \text{ keV}$ ). The isomer was produced and spin-aligned via a projectile-fragmentation reaction at intermediate energy, the Time Dependent Perturbed Angular Distribution (TDPAD) method being used for the measurement of the g factor. For the first time, due to significant improvements of the experimental technique, an appreciable residual alignment of the isomer has been observed, allowing a precise determination of its g factor:  $g = -0.229(2)$ . Comparison of the experimental g factor with shell-model and mean field calculations confirms the  $9/2^+$  spin and parity assignments and suggests the onset of deformation due to the intrusion of Nilsson orbitals emerging from the  $\nu g_{9/2}$ .

PACS numbers: 21.10.Ky, 21.60.-n, 23.20.En, 25.70.Mn

The measurement of electromagnetic (EM) moments has traditionally played a central role in the critical evaluation of nuclear structure models since they elucidate the single-particle nature (magnetic moments) and the shape (quadrupole moments) of the nuclear state under investigation. Their particular behavior around nuclear shell closures, approaching Schmidt values for magnetic moments and small values for quadrupole moments, makes them good tools to investigate shell closure near and far from  $\beta$  stability.

One of the main restrictions in the study of EM moments is the necessity to obtain oriented isomeric ensembles. In particular, for the study of neutron rich nuclei, that are mostly produced via fragmentation reactions at high or intermediary energies, the mechanism to produce oriented states is not yet well understood. The first observation of spin alignment of isomeric states in a projectile-fragmentation reaction at an energy of 500 MeV/u was reported by Schmidt-Ott *et al* [1]. At projectile energies below 100 MeV/u, so called intermediate energies, spin alignment of isomeric beams was reported recently by Georgiev *et al* [2] in the study of isomeric states in the  $^{68}\text{Ni}$  region. However, only a very small residual alignment observed in the decay of the  $^{67}\text{Ni}$  and the  $^{69}\text{Cu}$  isomers was reported.

In this letter, we report an important experimental achievement in the study of EM moments of neutron rich isomers. For the first time, high quality data could be obtained for an isomer in the neutron rich  $^{61}\text{Fe}$  nucleus, located near the controversial N=40 subshell closure [3, 4, 5, 6, 7, 8].

We focus here on the role played by the  $\nu g_{9/2}$  orbital in the low-energy level structure of nuclei near  $N = 40$  in the particular case where this orbital manifests itself as an isomeric state. The  $^{61m}\text{Fe}$ , with 35 neutrons, is one of the lightest nuclei exhibiting such an isomeric state ( $T_{1/2} = 250(10) \text{ ns}$ ) at a rather low excitation energy ( $E^* = 861 \text{ keV}$ ). The  $9/2^+$  tentatively assigned spin and parity is based on systematics [9]. The measurement of the g factor of the isomeric state in  $^{61}\text{Fe}$  provides information about its structure and can also confirm the suggested spin/parity.

The nuclei of interest were produced following the fragmentation of a 54.7 MeV/u  $^{64}\text{Ni}$  beam accelerated at the GANIL facility, with a mean intensity of  $7 \cdot 10^{11}$  pps, impinging on a 97.6 mg/cm<sup>2</sup> thick  $^9\text{Be}$  target placed at the entrance of the LISE spectrometer [10]. In order to decrease the in-flight decay of the isomer, the detection setup (Fig. 1) was positioned at the first focal plane of the LISE spectrometer (time of flight  $\approx 200 \text{ ns}$ ). A 300  $\mu\text{m}$  thick removable silicon detector was used to optimize the selection of  $^{61}\text{Fe}$  fragments by means of energy-loss vs time-of-flight identification. Once the selection was performed, a 50  $\mu\text{m}$  thick plastic scintillator, placed in front of the catcher foil, was used to provide the  $t = 0$  signal for the subsequent TDPAD measurement. The choice of a thin plastic scintillator instead of a silicon detector was made for two reasons. First, the fragments are selected fully stripped with the LISE spectrometer and, in order to preserve the initial alignment until the eventual stop in a catcher foil, it is important to avoid as much as possible the capture of electrons that

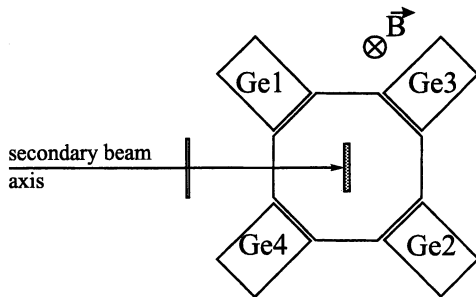


FIG. 1: Schematic drawing of the TDPAD experimental setup. The beam passes through a  $50 \mu\text{m}$  plastic scintillator before being stopped in a  $500 \mu\text{m}$  Cu foil.

can completely destroy the orientation of the nuclear ensemble. The electron pick-up upon passing through the scintillator is estimated to be below 2% [11], much lower than that in a  $300 \mu\text{m}$  thick silicon detector (60-70%) [2]. Secondly, the accepted secondary beam rate (between 17 and 80 kHz for the present experiment) can be one order of magnitude higher than with a silicon detector. As a catcher for the reaction products we used an annealed high-purity  $500 \mu\text{m}$  thick Cu foil. Iron ions have the same electronegativity and similar atomic radius as Cu atoms and hence Cu, with its cubic lattice structure, is expected to provide a perturbation-free environment for implanted Fe fragments. The Cu foil was placed between the poles of an electromagnet that provided a constant magnetic field  $\vec{B}$  in the vertical direction.

The Larmor precession of the initially aligned isomeric spins in the applied field of about 0.7 T, was monitored with four coaxial Ge detectors placed in the horizontal plane around the Cu foil as shown in Fig. 1. Time spectra were collected, having as start the signal due to the ion passage through the plastic scintillator and as stop the signal given by the detection of a prompt or delayed  $\gamma$ -ray. To extract the precession pattern out of the time spectra, data from detectors positioned at  $90^\circ$  with respect to each other was combined to generate the  $R(t)$ -function:

$$R(t) = \frac{I_{12}(\theta, t) - \epsilon I_{34}(\theta + \frac{\pi}{2}, t)}{I_{12}(\theta, t) + \epsilon I_{34}(\theta + \frac{\pi}{2}, t)} \sim A_2 B_2^0(t=0) \cos(2(\omega_L t + \alpha - \theta)). \quad (1)$$

with  $\vec{\omega}_L = -\frac{g\mu_N}{\hbar} \vec{B}$  and  $\alpha = -\frac{\pi}{2}(1 - \frac{gA}{2Z})$  both depending on the  $g$  factor.  $I_{12}$  and  $I_{34}$  are the summed intensities of detectors placed at 180 degrees (see figure 1);  $A_2$  is the radiation parameter of the  $\gamma$ -ray transition;  $B_2^0$  is the second component of the orientation tensor describing the initial orientation of the selected isomeric ensemble;  $\theta$  equals  $\pi/4$ ;  $\epsilon$  is the relative efficiency between the four respective detectors in the present setup, and  $\alpha$  is the rotation angle of the aligned ensemble symmetry axis with respect to the beam axis induced when passing through

the two dipole magnets of LISE spectrometer [2]. The data acquisition was validated on an event by event basis by the coincidence between a heavy ion signal from the plastic scintillator and a delayed  $\gamma$ , registered by one of the germanium detectors, within a time window of  $3 \mu\text{s}$ . In order to diminish the number of accidental coincidences in this time window, we have used a package suppresser that brought on target 1 out of 10 ion packages provided by the accelerator with a frequency of 10.5 MHz. As a consequence, the detected alignment increased by a factor of  $\sim 3$  compared to a measurement without package suppression.

Certain physical effects need to be taken into account when deducing a precise value for the  $g$  factor from the observed Larmor frequency. The distribution of the magnetic field over the beam spot, the paramagnetic amplification of the applied magnetic field and the Knight shift, all can induce minor modifications of the Larmor frequency. In order to avoid systematic errors due to these corrections and to validate the experimental setup and method, we have measured the Larmor precession under identical conditions for isomers in two Iron isotopes: the  $I^\pi = 10^+$ ,  $E^* = 6527 \text{ keV}$  isomer in  $^{54}\text{Fe}$  having a known  $g$  factor,  $g(10^+) = +0.7281(10)$  [12], and the  $I^\pi = (9/2^+)$ ,  $E^* = 861 \text{ keV}$  isomer in  $^{61}\text{Fe}$  decaying via a (M2) transition of 654 keV in cascade with a (M1) transition of 207 keV to the ground state (see fig. 2). The effective value of the magnetic field extracted from the  $R(t)$  function of  $^{54m}\text{Fe}$  (eq. 1) is 6800(40) Gs and it includes all the corrections mentioned above.

$^{54m}\text{Fe}$ , decaying by a stretched E2-cascade, served also as a probe to measure the produced alignment of the isomeric ensembles as a function of their angular momentum distribution [13]. For the selection of the fragments in the wing of the momentum distribution ( $p_{\text{fragment}} < p_{\text{projectile}}$ ), the amplitude of the  $R(t)$  function (fig. 2) yields a large negative alignment,  $-12.5(9)\%$ , the sign being in agreement with the predictions of a kinematical fragmentation model [14, 15].

For  $^{61m}\text{Fe}$ , we have studied the alignment for two ensembles selected, respectively, in the center and in the outer wing of the longitudinal momentum distribution. The alignment of the isomeric state, deduced from the amplitude of the  $R(t)$  functions of the 654 keV decay is  $+6.2(7)\%$  for the central selection and  $-15.9(8)\%$  for the wing selection, assuming a pure M2 transition.

The  $R(t)$  functions of the 207 keV and the 654 keV  $\gamma$ -rays de-exciting the  $^{61m}\text{Fe}$  isomer exhibit an opposite phase and the ratio between their amplitudes is 1.43(16). Using realistic GEANT simulations [16] and assuming that the 654 keV and 207 keV transitions have pure M2 and M1 multiplicities, respectively, and the level sequence is  $9/2^+ \rightarrow 5/2^- \rightarrow 3/2^-$ , we estimated this ratio to be 1.30(6). A spatial distribution close to the fragmented beam spot of the emitting  $^{61}\text{Fe}$  isomers is assumed as well in order to take into account the geometrical factor

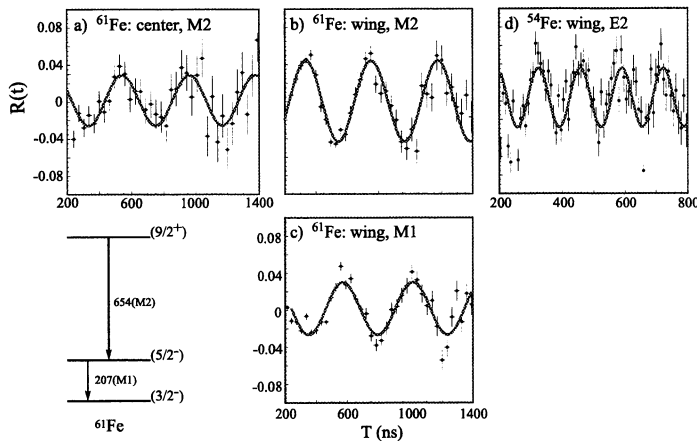


FIG. 2: The  $R(t)$  functions for: a.  ${}^{61}\text{Fe}$ (center, 654 keV); b.  ${}^{61}\text{Fe}$ (wing, 654 keV); c.  ${}^{61}\text{Fe}$ (wing, 207 keV); d.  ${}^{54}\text{Fe}$ . The  $R(t)$  function for 207 keV is consistent with that for the 654 keV but with opposite phase, as expected from the assumed multipolarities of the corresponding  $\gamma$  transitions.

of the detection setup. The good agreement between the two ratios (experimental and simulated) indicates that the multipolarities and sequence of the  $\gamma$  transitions used for the determination of the experimental alignment are correct.

The measured half-life of the  ${}^{61}\text{Fe}$  isomer,  $T_{1/2} = 245(5)$  ns, is in good agreement with the previous measurements [9]. For the  $g$  factor, a value of  $-0.229(2)$  was extracted by a  $\chi^2$  fit of the  $R(t)$  functions using expression (1) with both frequency and initial phase,  $\alpha$ , depending explicitly on  $g$ . The error on the fitted  $g$  factor includes the errors on the effective field. The fitted  $R(t)$  functions were constructed using the 654 keV direct decay of the isomeric state for the central and wing selection of the fragments momentum, respectively (fig. 2).

In Fig. 3 we present the measured  $g$  factors of  $9/2^+$  isomeric states around  $N = 40$ , including also the  $g$  factor of  ${}^{61m}\text{Fe}$ . The comparison with the other  $g$  factors of known  $9/2^+$  isomeric states in the region strongly supports the  $9/2^+$  spin and parity assignment for the  ${}^{61m}\text{Fe}$  isomer. One can observe the symmetry with respect to  $Z = 28$  of the  $g$  factors for  $N = 35$  chain and the increase of  $g$  factor values when one goes away from  $Z = 28$ , indicating an increase of core polarization effects.

In order to extract detailed information about the valence orbital occupation for the isomeric state, we have performed large scale shell model (LSSM) and mean-field calculations using the Hartree-Fock-Bogoliubov (HFB) formalism with an effective D1S Gogny nucleon-nucleon force [19].

The shell model calculations were performed using the ANTOINE code [20] of the Strasbourg group in a valence space composed of  $f, p$  and  $g_{9/2}$  active orbitals and having a closed  ${}^{48}\text{Ca}$  core. The interaction used is described in

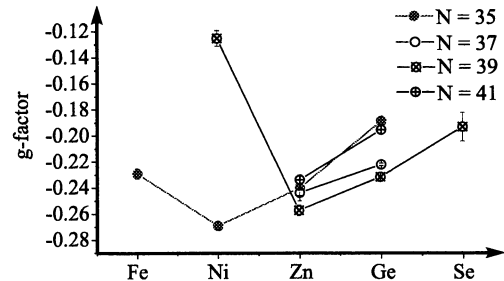


FIG. 3:  $g$  factor systematics around  $N=40$  for known  $9/2^+$  isomeric states. The data are taken from [2, 17, 18]. The unusual value for the  $g$  factor of  ${}^{67}\text{Ni}$  could be explained by proton excitations across  $Z=28$ .

[8] and in the references therein.

The calculated free  $g$  factor is  $g(9/2^+) = -0.277$ . The effective value is  $g(9/2^+) = -0.1828$  if a quenching factor of 0.7 is used for the nucleon spin  $g$  factor. The value of the quenching factor is quite arbitrary because at present there is no systematical comparison between experimental data and shell model calculations into the considered space. Recently, it was shown that for the  $sd$  and  $pf$  shells, the configuration mixing within the shells is enough to fully account for the observed magnetic moment, without the use of the quenching factor needed for Gamow-Teller beta decay [21]. The  $9/2^+$  state is calculated to be at 720 keV and its wave function is a mixture of a large number of configurations, but the mean occupation of the  $\nu g_{9/2}$  orbital is  $\approx 1$ . The good agreement between the calculated and the experimental value of the  $g$  factor indicates that the isomer is a  $9/2^+$  state, generated by a neutron in the  $\nu g_{9/2}$  orbital whilst its very mixed wave function could be related to a deformed potential.

For a better understanding of the variation of the single particle orbitals near the Fermi surface as a function of the nuclear deformation, we have calculated the ground-state and excited states within the Hartree-Fock-Bogoliubov (HFB) formalism. The calculation beyond the mean-field approximation was performed using the Generator Coordinate Method (GCM) with the Gaussian Overlap Approximation [22]. The ground state is found to be a  $K^\pi = 3/2^-$  prolate deformed state,  $\beta_2 = 0.187$ , whereas an excited state  $K^\pi = 9/2^+$  is predicted with an excitation energy  $E^* = 1640$  keV and an oblate deformation,  $\beta_2 = -0.227$ . Fig. 4 presents the HFB energies of the states located near the Fermi level in  ${}^{61}\text{Fe}$  as a function of the deformation parameter,  $\beta_2$ .

The free  $g$  factor of the  $J^\pi = 9/2^+$  state built from the  $K^\pi = 9/2^+$  HFB state is found to be  $g(9/2^+) = -0.3477$  (without a quenching factor) and it remains practically unchanged after applying the GCM method.

The comparison between the experimental value and the theoretical predictions, LSSM and HFB, indicates a deformed potential for the  $9/2^+$  isomeric state. One

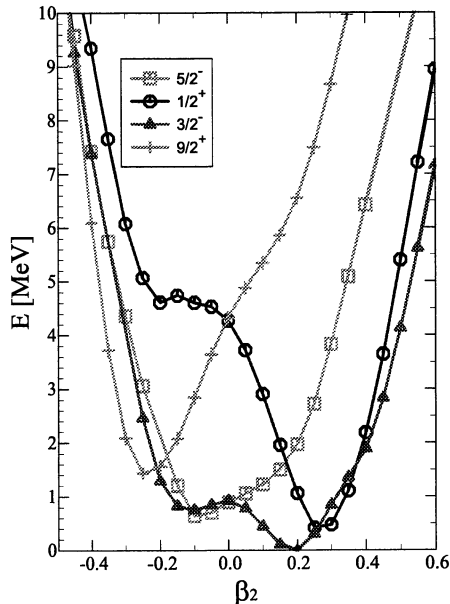


FIG. 4: Potential energy curves of the ground state and of the first three excited states of  $^{61}\text{Fe}$  as functions of the deformation parameter,  $\beta_2$ .

can notice that the two extreme HF orbitals ( $9/2^+$  and  $1/2^+$ ) generating from the spherical  $\nu g_{9/2}$  orbital (fig. 4) are close to the Fermi surface at moderate deformations but with opposite sign. In the one particle plus rotor model [23], this particularity provides two possible ways of creating a  $J^\pi = 9/2^+$  state, depending on how the unpaired neutron is coupled to the rotating  $^{60}\text{Fe}$  core. In the strong coupling scheme [24], the unpaired neutron spin couples to the deformation of the core and the  $9/2^+$  state has the projection on the symmetry axis  $K = 9/2$ . The second possibility is that the unpaired neutron spin couples to the rotation of the core and the total spin projection on the symmetry axis is degenerated between  $K = 1/2$  and  $K = -1/2$  due to the Coriolis interaction, so  $K$  is no longer a good quantum number. Instead, the projection on the rotation axis becomes a good quantum number and the spin of the physical state can be  $9/2^+$ . We have then calculated the low energy states in the frame of this model for  $^{61}\text{Fe}$ . Taking the deformations indicated by the HFB calculations, for the two cases presented above, the lowest state having a positive parity has a  $9/2$  spin and an excitation energy of about 850 keV. The  $g$  factors are similar, which was predictable because the  $g$  factor should not be sensitive to the deformation.

In conclusion, the measured  $g$  factor is in very good agreement with the assigned  $9/2^+$  spin and parity. From the comparison with LSSM and HFB calculations there are indications that this state is characterized by a deformed potential, induced by a steep lowering of the Nilsson orbitals emerging from the spherical  $\nu g_{9/2}$  neutron orbital as a function of deformation parameter,  $\beta_2$ . In

order to understand the coupling of the unpaired particle to the  $^{60}\text{Fe}$  core, it is important to measure the sign of the quadrupole moment of the isomeric state, requiring a spin polarized isomeric beam [25, 26].

The appreciably large residual alignment measured for the  $^{61}\text{Fe}$  and  $^{54}\text{Fe}$  fragments indicates that fragmentation reactions at intermediate energies can provide a powerful tool to align ensembles of nuclear isomers of yet more exotic nuclei, thus facilitating the determination of EM moments in neutron rich nuclei and allowing the investigation of nuclear structure away from stability.

We are grateful for the technical support received from the staff of the GANIL facility. This work has been partially supported by the Access to Large Scale Facility program under the TMR program of the EU, under contract nr. HPRI-CT-1999-00019, the INTAS project nr. 00-0463 and the IUAP project P5/07 of the Belgian Science Policy Office. We are grateful to the IN2P3/EPSRC French/UK loan pool for providing the Ge detectors. The Weizmann group has been supported by the Israel Science Foundation. G.N. and D.B. acknowledge the FWO-Vlaanderen for financial support.

- 
- [1] W.-D. Schmidt-Ott *et al.*, Z. Phys. **A350** (1994) 215.
  - [2] G. Georgiev *et al.*, Journ. of Physics **G28** (2002) 2993.
  - [3] M. Bernas *et al.*, Phys. Lett. **B113** (1982) 279.
  - [4] A.M. Oros-Peusquens *et al.*, Nucl. Phys. **A669** (2000) 81.
  - [5] R. Broda *et al.*, Phys. Rev. Lett. **74** (1995) 868.
  - [6] S. Leenhardt *et al.*, Eur. Phys. J. **A14** (2002) 1.
  - [7] K.-H. Langanke *et al.*, Phys. Rev. **C67** (2003) 044314.
  - [8] O. Sorlin *et al.*, Phys. Rev. Lett. **88** (2002) 092501-1.
  - [9] R. Grzywacz *et al.*, Phys. Rev. Lett. **81** (1998) 766.
  - [10] R. Anne *et al.*, Nucl. Instr. and Meth. in Phys. Res. **A257** (1987) 215.
  - [11] D. Bazin *et al.*, Nucl. Instr. and Meth. in Phys. Res. **A482** (2002) 307.
  - [12] M.H. Rafailovich *et al.*, Phys. Rev. **C27** (1983) 602.
  - [13] G. Neyens, Rep. Prog. Phys. **66** (2003) 633.
  - [14] K. Asahi *et al.*, Phys. Rev. **C43** (1991) 456.
  - [15] J.M. Daugas *et al.*, Phys. Rev. **C63** (2001) 064609.
  - [16] *GEANT - Detector Description and Simulation Tool* <http://wwwasdoc.web.cern.ch/wwwasdoc/>
  - [17] P. Raghavan, At. Data Nucl. Data Tables **42** (1989) 189.
  - [18] W. Müller *et al.*, Phys. Rev. **B40** (1989) 7633.
  - [19] J. Dechargé and D. Gogny, Phys. Rev. **C21** (1980) 1568.
  - [20] E. Caurier, shell model code ANTOINE, IRES, Strasbourg, 1989-2002.
  - [21] M. Honma *et al.*, Phys. Rev. **C69** (2004) 034335-1.
  - [22] J. Libert *et al.*, Phys. Rev. **C60** (1999) 054301.
  - [23] F. Stephens *et al.*, Phys. Rev. Lett. **29** (1972) 438.
  - [24] S.G. Nilsson and I. Ragnarsson, *Shapes and Shells in Nuclear Structure*, Cambridge University Press 1995, p 193.
  - [25] E. Dafni *et al.*, Phys. Rev. Lett. **53** (1984) 2473.
  - [26] M. Hass *et al.*, Nucl. Phys. **A414** (1984) 316.